

# Capture Region of a Three Dimensional PPN Guidance Law Against a High Speed-Nonmaneuvering Target

Feng Tyan and Jeng Fu Shen

**Abstract**—The three dimensional PPN guidance against a high speed-nonmaneuvering target is analyzed. A necessary and sufficient conditions for the missile to capture the target are obtained. The result is more general than those which presented previously. Furthermore, the capture region and criterion of finite LOS turn rate are found and shown in three-dimensional plots for a clear view.

**Keywords:** PPN missile guidance, high speed target, capture region

## I. INTRODUCTION

Capturing ballistic targets has been a challenge for missile guidance. It has been worked out by intensive simulation studies that the near-head-on scenery is the best way for a missile to capture a high speed target [1]. Therefore, there are several works that proposed missile guidance to achieve “head-on-attack” [2, 3]. However a question arises: what is the capturability of PPN, one of the most general and practical guidance law, to capture an extremely high speed target? We are going to answer the question in this work.

In the literature, there are many remarkable works studied the PPN, such as [4–7]. Guelman gave the qualitative analysis of PPN and Becker solved the closed-form solution for nonmaneuvering target. In addition, Ghose extended the analysis of Guelman to time-varying maneuvering target. While above works analyzed the capturability of two dimensional PPN, Ha and Tyan [8] worked on three dimensional ones. Ha, et al. [6] studied the performance of 3D PPN law against a high speed maneuvering target by introducing a Lyapunov-like approach. The analysis is performed in a so-called LOS plane. The result, however, is quite limited with the assumption that the target has a speed lower than that of the missile. The “high speed target” therein referred to a target that has a speed greater than  $1/\sqrt{2}$  times the speed of missile. Furthermore, the capturability (interceptibility) concluded from Lyapunov-like approach is conservative; since Lyapunov function tells about only sufficiency instead of necessity. A more general study of 3D PPN has been proposed by Tyan [8]. With the aid of a modified polar coordinate, 3D missile guidance laws have been studied under an unified approach. For a missile guided by PPN to capture a target from any initial aspect, having a speed higher than that of target is one of the sufficient conditions. Recently, several

works used the Frenet apparatus to formulate the guidance problem by the notion of differential geometry and proposed geometric guidance [9, 10]. By using Frenet apparatus, the equations describing relative dynamics of guidance problem become simple and the closed-form solution can be obtained. Above works, however, held the assumption that the target has a speed smaller than that of the missile.

We are, therefore, going to analyze the capturability of PPN against extremely high speed target by taking advantage of Frenet frame. Both necessary and sufficient conditions are explained by using a simple geometry; thus the result is more general than that of a Lyapunov-like approach. Specifically, while the target has a speed higher than that of the missile, the navigation constant of PPN should be at least greater than 4 for the missile to capture the target with finite LOS turn rate. Furthermore, the capture region as well as criterion of finite LOS turn rate are sketched in three dimensional plots for a concise view.

This paper is organized as follows. Section II reviews the relative dynamics of PPN in 3D space via the unified approach proposed in [8]. In the presence of a LOS fixed coordinate [11], equations demanded to implement 3D PPN law are derived. Having materials in hand, section III studies the capturability of PPN law against a high speed-nonmaneuvering target. The analysis is concluded as a necessary and sufficient condition of the capture region given in the main theorem. In addition, the capture region and the criterion of finite LOS turn rate are also revealed therein.

## II. PRELIMINARIES

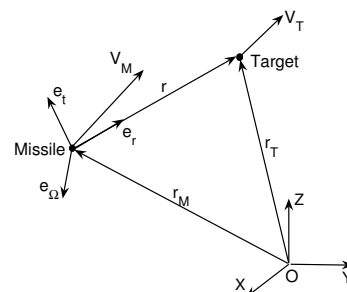


Fig. 1. LOS Fixed Coordinate

The relative dynamics of guidance problem can be expressed in a line-of-sight (LOS) fixed coordinate [11] as

Feng Tyan is a faculty with Computational Dynamics and Control Lab, Department of Aerospace Engineering, TamKang University, Taipei County 25147, Taiwan, R.O.C. Email: tyanfeng@mail.tku.edu.tw

Jeng Fu Shen is a research assistant with Computational Dynamics and Control Lab, Department of Aerospace Engineering, TamKang University, Taipei County 25147, Taiwan, R.O.C.

shown in Fig. 1. Assuming that missile and target are particles in the space, LOS vector can be defined as

$$\mathbf{r} \triangleq \mathbf{r}_T - \mathbf{r}_M \triangleq \rho \mathbf{e}_r, \quad (1)$$

where vectors  $\mathbf{r}_T$  and  $\mathbf{r}_M$  are position vectors of target and missile, respectively, in the reference frame. Range between target and missile is denoted by  $\rho$ , and  $\mathbf{e}_r$  is the unit vector in the direction of LOS. Relative velocity and acceleration can be represented as

$$\dot{\mathbf{r}} = \dot{\rho} \mathbf{e}_r + \rho \dot{\mathbf{e}}_r = \mathbf{v}_T - \mathbf{v}_M, \quad (2)$$

$$\ddot{\mathbf{r}} = \ddot{\rho} \mathbf{e}_r + 2\dot{\rho} \dot{\mathbf{e}}_r + \rho \ddot{\mathbf{e}}_r = \mathbf{a}_T - \mathbf{a}_M, \quad (3)$$

where  $\mathbf{v}_T$ ,  $\mathbf{a}_T$ ,  $\mathbf{v}_M$  and  $\mathbf{a}_M$  are velocity and acceleration vectors of target and missile, respectively. Assuming that the angular velocity vector of LOS,  $\boldsymbol{\Omega}$ , is orthogonal to LOS and

$$\boldsymbol{\Omega} = \mathbf{e}_r \times \dot{\mathbf{e}}_r, \quad (4)$$

then a coordinate system  $(\mathbf{e}_r, \mathbf{e}_t, \mathbf{e}_\Omega)$  can be defined, where

$$\mathbf{e}_t \triangleq \frac{\dot{\mathbf{e}}_r}{\|\boldsymbol{\Omega}\|}, \quad \mathbf{e}_\Omega \triangleq \frac{\boldsymbol{\Omega}}{\|\boldsymbol{\Omega}\|}. \quad (5)$$

By using the  $(\mathbf{e}_r, \mathbf{e}_t, \mathbf{e}_\Omega)$  frame (Frenet frame), a set of three scalar differential equations

$$\frac{d}{dt} \dot{\rho} = \rho \|\boldsymbol{\Omega}\|^2 + (a_{T_r} - a_{M_r}), \quad \dot{\rho}(t_0) = \dot{\rho}_0,$$

$$\frac{d}{dt} \rho \|\boldsymbol{\Omega}\| = -\dot{\rho} \|\boldsymbol{\Omega}\| + (a_{T_t} - a_{M_t}), \quad \rho \|\boldsymbol{\Omega}\|(t_0) = \rho \|\boldsymbol{\Omega}\|_0,$$

$$\frac{d}{dt} \rho = \dot{\rho}, \quad \rho(t_0) = \rho_0,$$

is obtained to describe the relative dynamics of guidance problem in three dimensional space. Note that the subscript indices of  $\mathbf{a}_M$  and  $\mathbf{a}_T$  denote representations in  $(\mathbf{e}_r, \mathbf{e}_t, \mathbf{e}_\Omega)$  frame. For more details of above approach, reader may refer to [11]. To save space only brief review is mentioned.

The PPN law [8] is given as

$$\mathbf{a}_M = \beta \boldsymbol{\Omega} \times V_M \mathbf{e}_{vM}, \quad (6)$$

where  $\beta$  is the navigation constant,  $V_M$  the speed of missile and  $\mathbf{e}_{vM}$  the unit velocity vector of missile. With assumption that target has no maneuver, namely  $\mathbf{a}_T = 0$ ; definition of variables

$$u \triangleq \dot{\rho} \quad v \triangleq \rho \|\boldsymbol{\Omega}\| \quad w \triangleq \frac{1}{\rho}; \quad (7)$$

transformation of independent variable from  $t$  to  $\tau$  by  $d\tau = u dt$ ; dynamic equations of PPN law are given as

$$\frac{du}{d\tau} = [v + \beta V_M (\mathbf{e}_{vM}^T \mathbf{e}_t)] v, \quad u(\tau_0) = u_0, \quad (8a)$$

$$\frac{dv}{d\tau} = [-u - \beta V_M (\mathbf{e}_{vM}^T \mathbf{e}_r)] v, \quad v(\tau_0) = v_0, \quad (8b)$$

$$\frac{dw}{d\tau} = -uw, \quad w(\tau_0) = w_0, \quad (8c)$$

and

$$\begin{aligned} \frac{d}{d\tau} (\mathbf{e}_{vM}^T \mathbf{e}_r) &= -(\beta - 1) (\mathbf{e}_{vM}^T \mathbf{e}_t) v, \\ (\mathbf{e}_{vM}^T \mathbf{e}_r)(\tau_0) &= (\mathbf{e}_{vM}^T \mathbf{e}_r)_0, \end{aligned} \quad (9a)$$

$$\begin{aligned} \frac{d}{d\tau} (\mathbf{e}_{vM}^T \mathbf{e}_t) &= (\beta - 1) (\mathbf{e}_{vM}^T \mathbf{e}_r) v, \\ (\mathbf{e}_{vM}^T \mathbf{e}_t)(\tau_0) &= (\mathbf{e}_{vM}^T \mathbf{e}_t)_0, \end{aligned} \quad (9b)$$

$$\begin{aligned} \frac{d}{d\tau} (\mathbf{e}_{vM}^T \mathbf{e}_\Omega) &= 0, \quad (\mathbf{e}_{vM}^T \mathbf{e}_\Omega)(\tau_0) = (\mathbf{e}_{vM}^T \mathbf{e}_\Omega)_0. \end{aligned} \quad (9c)$$

Note that  $u$  is constant when  $v$  goes to zero; since  $v = 0$  implies  $du/d\tau = dv/d\tau = 0$ . Equations (9) reveals that

$$\begin{bmatrix} (\mathbf{e}_{vM}^T \mathbf{e}_r)(\theta) \\ (\mathbf{e}_{vM}^T \mathbf{e}_t)(\theta) \end{bmatrix} = R[(\beta - 1)(\theta - \theta_0)] \begin{bmatrix} (\mathbf{e}_{vM}^T \mathbf{e}_r)_0 \\ (\mathbf{e}_{vM}^T \mathbf{e}_t)_0 \end{bmatrix}, \quad (10)$$

where  $\theta$  is defined by  $d\theta = v d\tau$ , and

$$R[\cdot] \triangleq \begin{bmatrix} \cos(\cdot) & -\sin(\cdot) \\ \sin(\cdot) & \cos(\cdot) \end{bmatrix}. \quad (11)$$

Note that direction cosines  $(\mathbf{e}_{vM}^T \mathbf{e}_r)$ ,  $(\mathbf{e}_{vM}^T \mathbf{e}_t)$  and  $(\mathbf{e}_{vM}^T \mathbf{e}_\Omega)$  satisfy

$$(\mathbf{e}_{vM}^T \mathbf{e}_r)^2(\theta) + (\mathbf{e}_{vM}^T \mathbf{e}_t)^2(\theta) + (\mathbf{e}_{vM}^T \mathbf{e}_\Omega)^2(\theta) = 1. \quad (12)$$

Together with equation (10) and the facts

$$\begin{aligned} u &= V_T (\mathbf{e}_{vT}^T \mathbf{e}_r) - V_M (\mathbf{e}_{vM}^T \mathbf{e}_r), \\ v &= V_T (\mathbf{e}_{vT}^T \mathbf{e}_t) - V_M (\mathbf{e}_{vM}^T \mathbf{e}_t), \end{aligned} \quad (13)$$

where  $\mathbf{e}_{vT}$  is unit velocity vector of target, (8a) and (8b) can be solved to obtain

$$\begin{aligned} \begin{bmatrix} u(\theta) \\ v(\theta) \end{bmatrix} &= R[-(\theta - \theta_0)] \begin{bmatrix} V_T (\mathbf{e}_{vT}^T \mathbf{e}_r)_0 \\ V_T (\mathbf{e}_{vT}^T \mathbf{e}_t)_0 \end{bmatrix} \\ &\quad + R[(\beta - 1)(\theta - \theta_0)] \begin{bmatrix} V_M (\mathbf{e}_{vM}^T \mathbf{e}_r)_0 \\ V_M (\mathbf{e}_{vM}^T \mathbf{e}_t)_0 \end{bmatrix}, \end{aligned} \quad (14)$$

where  $(\mathbf{e}_{vT}^T \mathbf{e}_r)(\theta_0) \triangleq (\mathbf{e}_{vT}^T \mathbf{e}_r)_0$ ,  $(\mathbf{e}_{vT}^T \mathbf{e}_t)(\theta_0) \triangleq (\mathbf{e}_{vT}^T \mathbf{e}_t)_0$ . Therefore, equations (10), (13) and (14) yield that

$$\begin{bmatrix} (\mathbf{e}_{vM}^T \mathbf{e}_r)(\theta) \\ (\mathbf{e}_{vM}^T \mathbf{e}_t)(\theta) \end{bmatrix} = R[-(\theta - \theta_0)] \begin{bmatrix} (\mathbf{e}_{vM}^T \mathbf{e}_r)_0 \\ (\mathbf{e}_{vM}^T \mathbf{e}_t)_0 \end{bmatrix}. \quad (15)$$

Reader may refer to [8] for more details of above results. These equations will be used in the analysis of next section.

### III. CAPTURABILITY ANALYSIS OF PPN AGAINST HIGH SPEED-NONMANEUVERING TARGET

Define the normalized variables

$$\bar{u} \triangleq \frac{u}{V_T}, \quad \bar{v} \triangleq \frac{v}{V_T}, \quad (16)$$

then equation (14) can be written as

$$\begin{aligned} \begin{bmatrix} \bar{u}(\theta) \\ \bar{v}(\theta) \end{bmatrix} &= R[-(\theta - \theta_0)] \begin{bmatrix} (\mathbf{e}_{vM}^T \mathbf{e}_r)_0 \\ (\mathbf{e}_{vM}^T \mathbf{e}_t)_0 \end{bmatrix} \\ &\quad + R[(\beta - 1)(\theta - \theta_0)] \begin{bmatrix} \mu (\mathbf{e}_{vM}^T \mathbf{e}_r)_0 \\ \mu (\mathbf{e}_{vM}^T \mathbf{e}_t)_0 \end{bmatrix}, \end{aligned} \quad (17)$$

where

$$\mu \triangleq V_M / V_T.$$

Since this work concerns with high speed target; reader may keep in mind that  $\mu \leq 1$  in the following analysis. By defining

$$\begin{aligned} x &\triangleq \sqrt{(\mathbf{e}_{vM}^T \mathbf{e}_r)_0^2 + (\mathbf{e}_{vM}^T \mathbf{e}_t)_0^2} = \sqrt{1 - (\mathbf{e}_{vM}^T \mathbf{e}_\Omega)_0^2}, \\ y &\triangleq \sqrt{(\mathbf{e}_{vT}^T \mathbf{e}_r)_0^2 + (\mathbf{e}_{vT}^T \mathbf{e}_t)_0^2} = \sqrt{1 - (\mathbf{e}_{vT}^T \mathbf{e}_\Omega)_0^2}, \end{aligned} \quad (18)$$

and

$$\begin{aligned} \cos(\theta_{vT0}) &= \frac{(\mathbf{e}_{vT}^T \mathbf{e}_r)_0}{y}, \quad \cos(\theta_{vM0}) = \frac{(\mathbf{e}_{vM}^T \mathbf{e}_r)_0}{x}, \\ \sin(\theta_{vT0}) &= \frac{(\mathbf{e}_{vT}^T \mathbf{e}_t)_0}{y}, \quad \sin(\theta_{vM0}) = \frac{(\mathbf{e}_{vM}^T \mathbf{e}_t)_0}{x}, \end{aligned} \quad (19)$$

$\bar{u}$  and  $\bar{v}$  can be written as

$$\begin{aligned} \bar{u} &= y \cos(\theta_{vT0} - \Delta\theta) - \mu x \cos(\theta_{vM0} + (\beta - 1)\Delta\theta), \\ \bar{v} &= y \sin(\theta_{vT0} - \Delta\theta) - \mu x \sin(\theta_{vM0} + (\beta - 1)\Delta\theta), \end{aligned} \quad (20)$$

where  $\Delta\theta$  denotes  $\theta - \theta_0$  for terseness. The capture region of PPN law against a high speed-nonmaneuvering target is defined as follows.

**Definition 3.1:** Capture region  $\mathcal{C}\mathcal{R}_{PPN}$  of PPN law is the set of initial conditions such that there exist a  $\theta_f$  satisfies (21) the following capture condition [8],

$$\bar{u}_f \triangleq \bar{u}(\theta_f) < 0, \quad \bar{v}_f \triangleq \bar{v}(\theta_f) = 0. \quad (21)$$

It is reasonable to find  $\mathcal{C}\mathcal{R}_{PPN}$  with the aid of differential geometry since differential forms of  $\bar{u}$  and  $\bar{v}$  are involved to determine what direction and trajectory will be traversed by  $\bar{u}$  and  $\bar{v}$  on the  $(\bar{u}, \bar{v})$  plane. Trajectories of  $\bar{u}$  and  $\bar{v}$  on  $(\bar{u}, \bar{v})$  plane is realized as *Cycloids* as shown in figures 2 and 3 with variations of  $\beta$ ,  $\theta_{vT0}$  and  $\theta_{vM0}$ . As we can tell from Fig. 2, distinct  $\beta$  renders distinct type of cycloid while different set of  $(\theta_{vT0}, \theta_{vM0})$  renders different attitude and initial point of the same cycloid. Note that  $\bar{v} \geq 0$  by definition while the part  $\bar{v} < 0$  is drawn to give a whole view of trajectories. In general, there is no simple way to analyze  $\mathcal{C}\mathcal{R}_{PPN}$  by differential geometry due to the complexity comes from variations of  $\beta$ ,  $\theta_{vT0}$  and  $\theta_{vM0}$ .

However,  $(\bar{u}(\theta), \bar{v}(\theta))$  can also be realized as the subtraction of  $\mathbf{e}_{vT}$  and  $\mu\mathbf{e}_{vM}$  (realizations on  $(\bar{u}, \bar{v})$  plane), whose trajectories traverse two circles centered at the origin with radii  $y$  and  $\mu x$ . Equation (20) gives these two circles

$$\begin{aligned} \mathcal{C}_{\mathbf{e}_{vT}} &\triangleq (y \cos(\theta_{vT0} - \Delta\theta), y \sin(\theta_{vT0} - \Delta\theta)) \\ \mathcal{C}_{\mathbf{e}_{vM}} &\triangleq (\mu x \cos(\theta_{vM0} + (\beta - 1)\Delta\theta), \\ &\quad \mu x \sin(\theta_{vM0} + (\beta - 1)\Delta\theta)). \end{aligned}$$

Accordingly, going to zero of  $\bar{v}$  is equivalent to arriving at the same horizontal line of  $\mathbf{e}_{vT}$  and  $\mu\mathbf{e}_{vM}$ , to achieve this,

$$y \sin(\theta_{vT0} - \Delta\theta) = \mu x \sin(\theta_{vM0} + (\beta - 1)\Delta\theta). \quad (22)$$

The radii of  $\mathcal{C}_{\mathbf{e}_{vT}}$  and  $\mathcal{C}_{\mathbf{e}_{vM}}$  determine the possible region satisfies (22) on  $(\bar{u}, \bar{v})$  plane. To see this, first consider a fact that having no component in  $\mathbf{e}_\Omega$  direction of  $\mathbf{a}_M$  and  $\dot{\mathbf{r}}$  implies that

$$\begin{aligned} (\mathbf{e}_{vM}^T \mathbf{e}_\Omega)(\theta) &= (\mathbf{e}_{vM}^T \mathbf{e}_\Omega)(\theta_0), \quad \forall \theta, \\ (\mathbf{e}_{vT}^T \mathbf{e}_\Omega)(\theta) - \mu(\mathbf{e}_{vM}^T \mathbf{e}_\Omega)(\theta) &= 0, \quad \forall \theta. \end{aligned} \quad (23)$$

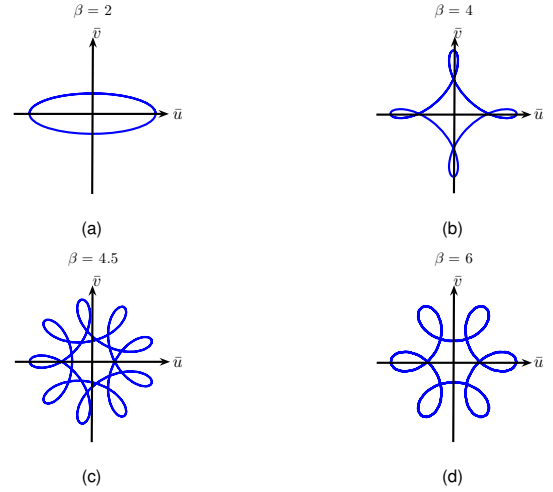


Fig. 2. Trajectories of  $(\bar{u}, \bar{v})$  with Variation of  $\beta$

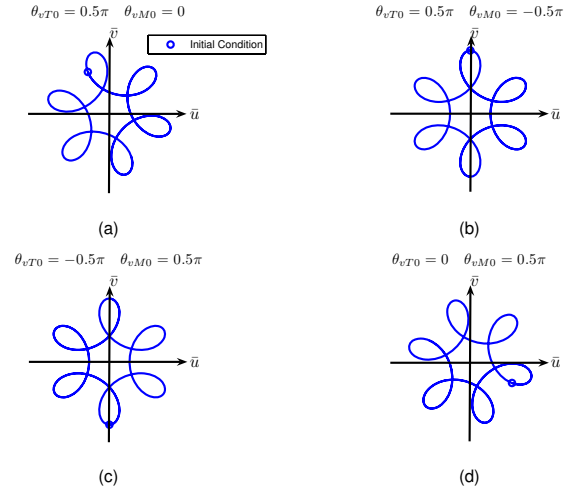


Fig. 3. Trajectories of  $(\bar{u}, \bar{v})$  with Variation of  $\theta_{vT0}$  and  $\theta_{vM0}$

Then the relation

$$\mu^2 - 1 = \mu^2 x^2 - y^2, \quad (24)$$

which indicates that  $y \geq \mu x$  as  $\mu \leq 1$ , is drawn. Consequently, as  $\mu < 1$ , the radius of  $\mathcal{C}_{\mathbf{e}_{vT}}$  is greater than that of  $\mathcal{C}_{\mathbf{e}_{vM}}$ . By using of simple geometry, it can be concluded that  $\bar{v} = 0$  occurs only if  $\mathbf{e}_{vT}$  is in the possible region shown in Fig. 4. Since  $\bar{u}_f < 0$  is required by capture condition (21), only the left-hand part of possible region is acceptable, which in turn implies that  $(\mathbf{e}_{vT}^T \mathbf{e}_r)(\theta_f) \triangleq (\mathbf{e}_{vT}^T \mathbf{e}_r)_f < 0$ .

As  $\Delta\theta > 0$  by definition, there are two cases of  $\beta$  under consideration. For  $\beta > 1$ ,  $\mathbf{e}_{vT}$  traverses  $\mathcal{C}_{\mathbf{e}_{vT}}$  clockwise while  $\mu\mathbf{e}_{vM}$  traverses  $\mathcal{C}_{\mathbf{e}_{vM}}$  counterclockwise. To satisfy (21) in this case, going to zero of  $\bar{v}$  comes before crossing through positive  $\bar{v}$  axis of  $\mu\mathbf{e}_{vM}$ , otherwise  $\bar{u}_f > 0$  when  $\bar{v}_f = 0$ . For  $\beta < 1$ , both  $\mathbf{e}_{vT}$  and  $\mu\mathbf{e}_{vM}$  traverse the circles clockwise. Again to satisfy (21), going to zero of  $\bar{v}$  comes before crossing through positive  $\bar{v}$  axis of  $\mathbf{e}_{vT}$  and  $\mu\mathbf{e}_{vM}$ , otherwise  $\bar{u}_f > 0$  when  $\bar{v}_f = 0$ . In the later case that  $\beta < 1$ ,

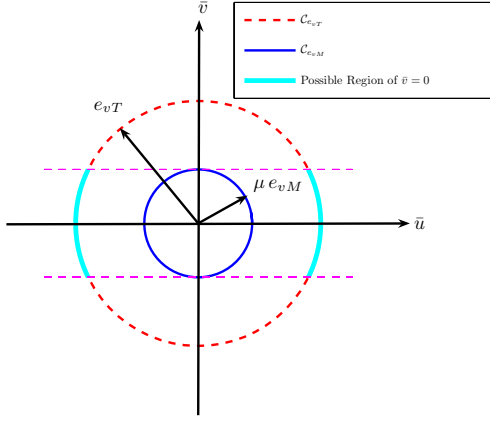


Fig. 4. Possible Region of  $\bar{v} = 0$

$(\mathbf{e}_{vM}^T \mathbf{e}_r)_f < 0$  when  $\bar{v}_f = 0$ , which is unfeasible in reality. Therefore,  $\beta < 1$  will no longer be considered in this work.

In short, for existence of a  $\theta_f$  such that condition (21) is satisfied, it is necessary that

$$-\mu x < (\mathbf{e}_{vT}^T \mathbf{e}_t)_0 < \mu x, \quad (\mathbf{e}_{vT}^T \mathbf{e}_r)_0 < 0, \quad (25)$$

or equivalently

$$\pi - \sin^{-1}(r_{PPN}) < \theta_{vT0} < \pi + \sin^{-1}(r_{PPN}), \quad (26)$$

where  $r_{PPN} \triangleq \frac{\mu x}{y} = \sqrt{\frac{\mu^2 + y^2 - 1}{y^2}}$ . Note that for  $r_{PPN}$  to exist,  $\mu$  and  $y$  must satisfy  $\mu^2 + y^2 \geq 1$ , which is equivalent of  $\mu \geq |(\mathbf{e}_{vT}^T \mathbf{e}_\Omega)_0|$ .

**Definition 3.2:** Given  $\mu$  and  $y$ ;  $\mathcal{S}_1$  is defined as

$$\mathcal{S}_1 \triangleq \left\{ \theta_{vT0} \mid \pi - \sin^{-1}(r_{PPN}) < \theta_{vT0} < \pi + \sin^{-1}(r_{PPN}) \right\}$$

Equations (12), (13) and (23) can be used to conclude that  $\bar{u}$ ,  $\bar{v}$ ,  $(\mathbf{e}_{vT}^T \mathbf{e}_r)$  and  $(\mathbf{e}_{vT}^T \mathbf{e}_t)$  satisfy

$$\left[ \bar{u} - (\mathbf{e}_{vT}^T \mathbf{e}_r) \right]^2 + \left[ \bar{v} - (\mathbf{e}_{vT}^T \mathbf{e}_t) \right]^2 = \mu^2 - (\mathbf{e}_{vT}^T \mathbf{e}_\Omega)_0^2. \quad (27)$$

By introduction of

$$(\mathbf{e}_{vT}^T \mathbf{e}_r)(\theta) = y \cos(\theta_{vT0} - \Delta\theta), \quad (28a)$$

$$(\mathbf{e}_{vT}^T \mathbf{e}_t)(\theta) = y \sin(\theta_{vT0} - \Delta\theta), \quad (28b)$$

equation (27) can be rearranged to yield

$$\left[ \frac{\bar{u}}{y} - \cos(\theta_{vT0} - \Delta\theta) \right]^2 + \left[ \frac{\bar{v}}{y} - \sin(\theta_{vT0} - \Delta\theta) \right]^2 = r_{PPN}^2. \quad (29)$$

**Definition 3.3:** Given  $\mu$  and  $y$ ;  $\mathcal{S}_2$  is defined as

$$\mathcal{S}_2 \triangleq \left\{ (\bar{u}, \bar{v}, \theta_{vT0}) \mid \bar{v} \geq 0, \mu^2 + y^2 \geq 1, r_{PPN}^2 = \left[ \frac{\bar{u}}{y} - \cos(\theta_{vT0} - \Delta\theta) \right]^2 + \left[ \frac{\bar{v}}{y} - \sin(\theta_{vT0} - \Delta\theta) \right]^2 \right\}$$

Note that  $y$  represents initial aspect in *third dimension*,  $\mathbf{e}_\Omega$ , instead of  $\mathbf{e}_r$  and  $\mathbf{e}_t$ .

**Remark 3.1:** If target has an extremely high speed relative to the speed of missile such that  $\mu \sim 0$ ; consequently  $\theta_{vT0} \sim \pi$  and  $y \sim 1$  are necessary for capture, which in turn is near head on scenario. Furthermore, the necessity that  $\mu \geq |(\mathbf{e}_{vT}^T \mathbf{e}_\Omega)_0|$  implies that 3D PPN will degenerate to a two dimensional one.

With definitions 3.2 and 3.3 in hand, capturability for PPN law can be summed up as follow.

**Theorem 3.1:** Consider a missile commanded by PPN law

$$\mathbf{a}_M = -\beta V_M \mathbf{e}_{vM} \times \boldsymbol{\Omega}. \quad (30)$$

To capture a high speed-nonmaneuvering target, it is necessary and sufficient that

$$\mathcal{CR}_{PPN} = \{(\bar{u}_0, \bar{v}_0, \theta_{vT0}) \mid \mathcal{S}_1 \cup \mathcal{S}_2\} \quad (31)$$

and

$$\beta \geq \frac{\frac{\pi}{2} \pm 2k\pi - \theta_{vM0}}{\theta_{vT0} + \sin^{-1}(r_{PPN}) - \pi} + 1, \quad (32)$$

where the choice of  $k$  depends on  $\theta_{vM0}$ .

Furthermore, with definitions

$$z_1 \triangleq \sin^{-1} \sqrt{\frac{(\bar{\beta} - 2)^2 r_{PPN}^2 - 4}{\bar{\beta}(\bar{\beta} - 4)}}, \quad (33)$$

$$z_2 \triangleq \sin^{-1} \sqrt{\frac{(\bar{\beta} - 2)^2 r_{PPN}^2 - 4}{\bar{\beta}(\bar{\beta} - 4) r_{PPN}^2}};$$

if  $\beta > \bar{\beta}$  where  $\bar{\beta}$  satisfies

$$\theta_{vT0} - \pi + z_1 = \frac{1}{\beta - 1} (z_2 - \theta_{vM0}), \quad (34)$$

finite LOS turn rate is retained.

*Proof:* The necessity is given previously. We are going to show the sufficiency. The last  $\theta$  for  $\bar{v}_f = 0$  and  $\bar{u}_f < 0$  is given by

$$\mu x \sin(\theta_{vM0} + (\beta - 1)(\bar{\theta} - \theta_0)) = \mu x, \quad (35a)$$

$$y \sin(\theta_{vT0} + (\bar{\theta} - \theta_0)) = \mu x. \quad (35b)$$

Equation (35) give

$$\bar{\theta} - \theta_0 = \frac{\frac{\pi}{2} \pm 2k\pi - \theta_{vM0}}{\beta - 1}, \quad (36a)$$

$$\bar{\theta} - \theta_0 = \theta_{vT0} + \sin^{-1}\left(\frac{\mu x}{y}\right) - \pi. \quad (36b)$$

Equating and rearranging of equations (36a) and (36b) yield

$$\beta = \frac{\frac{\pi}{2} \pm 2k\pi - \theta_{vM0}}{\theta_{vT0} + \sin^{-1}(r_{PPN}) - \pi} + 1. \quad (37)$$

Given  $\beta$  satisfies (37), there exists a  $\theta_f < \bar{\theta}$  such that  $\bar{v}_f = 0$  and  $\bar{u}_f < 0$ , as shown in Fig. 5. Because the larger  $\beta$  is, the smaller  $\theta_f - \theta_0$  will be, inequality (32) is concluded.

Now finite LOS turn rate is shown with assumption that initial conditions are in  $\mathcal{CR}_{PPN}$ . When  $\bar{v}_f = 0$ , equation (29) degenerates to

$$\left[ \frac{\bar{u}_f}{y} - \cos(\theta_{vT0} - \Delta\theta_f) \right]^2 + \sin^2(\theta_{vT0} - \Delta\theta_f) = r_{PPN}^2, \quad (38)$$

where  $\Delta\theta_f = \theta_f - \theta_0$ . After some arrangements, equation (38) is rearranged into

$$\bar{u}_f = y \cos(\theta_{vT0} - \Delta\theta_f) - y \sqrt{r_{PPN}^2 - \sin^2(\theta_{vT0} - \Delta\theta_f)}, \quad (39)$$

where the facts  $\bar{u}_f < 0$  and  $y \cos(\theta_{vT0} - \Delta\theta_f) < 0$  have been applied. It has been shown that  $-2\bar{u}_f - \beta\mu(e_{vM}^T e_r)_f \leq 0$  implies that  $\|\Omega\|(t_f) \leq \|\Omega\|(t_0)$  [8]; since

$$\rho \|\Omega\| \frac{-2\bar{u}_f - \beta\mu(e_{vM}^T e_r)_f}{-\bar{u}_f} = \text{constant}, \quad \text{for } \rho \|\Omega\| \rightarrow 0. \quad (40)$$

By using of equations (13) and (39),  $-2\bar{u}_f - \beta\mu(e_{vM}^T e_r)_f$  can be written as

$$-2y \cos(\theta_{vT0} - \Delta\theta_f) - (\beta - 2)y \sqrt{r_{PPN}^2 - \sin^2(\theta_{vT0} - \Delta\theta_f)}. \quad (41)$$

Suppose that  $\bar{\beta}$  satisfies (32) then there is a  $\delta$  such that

$$y \cos(\theta_{vT0} - \Delta\theta_f) = -\sqrt{1 - \mu^2} - \delta, \quad \delta > 0. \quad (42)$$

Thus (41) can be written as

$$2(\sqrt{1 - \mu^2} + \delta) - (\beta - 2)\sqrt{\delta^2 + 2\delta\sqrt{1 - \mu^2}}. \quad (43)$$

For (43) to be semi-negative, it is necessary and sufficient that

$$\delta \geq -\sqrt{1 - \mu^2} + \frac{(\bar{\beta} - 2)\sqrt{1 - \mu^2}}{\sqrt{\bar{\beta}(\bar{\beta} - 4)}}, \quad \bar{\beta} \geq 4. \quad (44)$$

By introducing minimum  $\delta$  into equation (42), it can be shown that

$$\begin{aligned} y^2 \sin^2(\theta_{vT0} - \Delta\theta_f) &= y^2 - y^2 \cos^2(\theta_{vT0} - \Delta\theta_f) \\ &= y^2 - \frac{(\bar{\beta} - 2)^2(1 - \mu^2)}{\bar{\beta}(\bar{\beta} - 4)}. \end{aligned} \quad (45)$$

By solving

$$\begin{aligned} y^2 \sin(\theta_{vT0} - \Delta\theta_f) &= y^2 - \frac{(\bar{\beta} - 2)^2(1 - \mu^2)}{\bar{\beta}(\bar{\beta} - 4)} \\ \mu^2 x^2 \sin(\theta_{vM0} + (\bar{\beta} - 1)\Delta\theta_f) &= y^2 - \frac{(\bar{\beta} - 2)^2(1 - \mu^2)}{\bar{\beta}(\bar{\beta} - 4)} \end{aligned}$$

and eliminating  $\Delta\theta_f$ , it can be concluded that  $\bar{\beta}$  satisfies equation (34). Therefore, inequality (44) is satisfied by choosing a  $\beta > \bar{\beta}$ , which in turn implies that (43) is semi-negative and hence, finite LOS turn rate is retained. ■

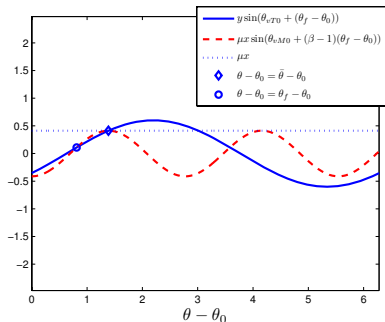


Fig. 5. Existence of  $\theta_f$

Fig. 6 shows capture region of PPN with  $y = 0.8$ . As we can tell, the larger  $\mu$  is, the larger capture region will be. Fig. 7 shows capture region of  $\mu = 0.8$  with distinct  $y$ . Fig. 8 shows level contours of  $\beta$  satisfy equation (37). Note that the figure is divided by  $\bar{v}_0 = 0$  (dashed line) into two parts  $\bar{v}_0 > 0$  and  $\bar{v}_0 < 0$ . Part  $\bar{v}_0 < 0$  is unacceptable. Only the range of  $\theta_{vT0}$  such that  $\theta_{vT0} \in \mathcal{S}_1$  is drawn. It can be seen, from this figure, large  $\beta$  is required when  $\theta_{vT0}$  is closed to  $\pi - \sin^{-1}(r_{PPN})$  and  $\theta_{vM0}$  is small, which confirms the geometric view in Fig. ???. Fig. 9 shows admissible region of finite LOS turn rate. It can be seen that when  $\theta_{vT0}$  is closed to  $\pi - \sin^{-1}(r_{PPN})$ , a larger  $\beta$  is demanded; on the contrary, if  $\theta_{vT0}$  is closed to  $\pi + \sin^{-1}(r_{PPN})$ , a smaller  $\beta$  is enough to achieve finite LOS turn rate.

**Concluding Remarks 3.1:** For a missile commanded by PPN to capture a high speed-nonmaneuvering target:

- The sufficiency is guaranteed by a  $\beta$  satisfies (32).
- The necessity is that the initial aspect of target on  $(\mathbf{e}_r, \mathbf{e}_t)$  plane,  $\theta_{vT0}$ , must be in the range of  $\pi \pm \sin^{-1}(r_{PPN})$ , and the range is limited by the speed ratio,  $\mu$ .
- To capture the high speed target with finite LOS turn rate, the navigation constant should be at least greater than 4.
- The admissible region for finite LOS turn rate is found as shown in Fig. 9.

In brief, capture region of PPN is quite limited if target has a speed higher than that of missile. And for a missile to capture a target that has an extremely high speed relative to that of missile; namely,  $\mu \sim 0$ , three dimensional space PPN degenerates to a two dimensional one; since  $\mu \geq |(\mathbf{e}_{vT}^T \mathbf{e}_\Omega)_0|$  is necessary.

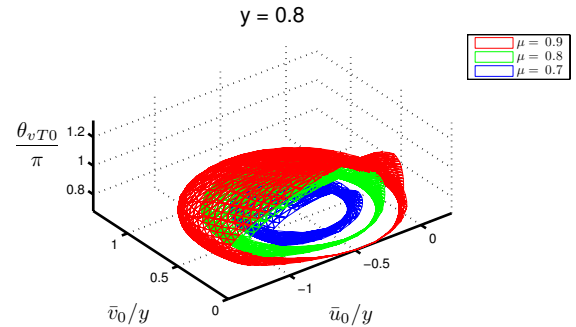


Fig. 6. Capture Region of PPN

## IV. CONCLUSIONS

In this work, the capturability of a 3D PPN guidance law against a high speed-nonmaneuvering target has been worked out. A necessary and sufficient condition for capture is concluded. In the next challenge, we are going to analyze the capturability of PPN in the presence of aerodynamic drag.

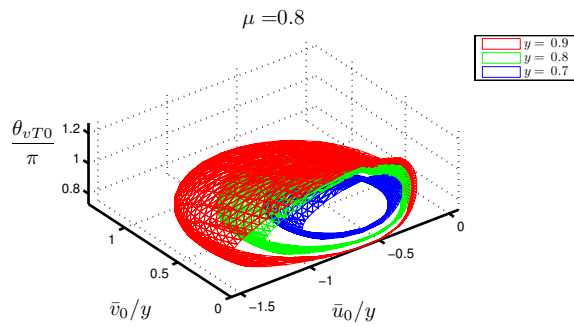


Fig. 7. Capture Region of PPN

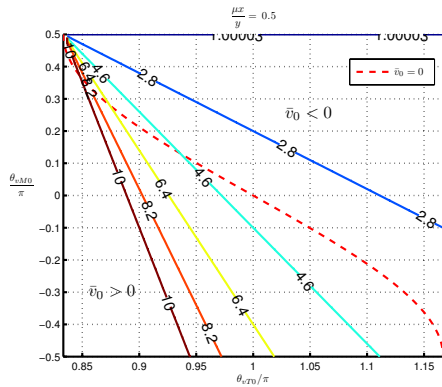


Fig. 8. Level Contours of  $\beta$  Respect to Initial Aspect Angles

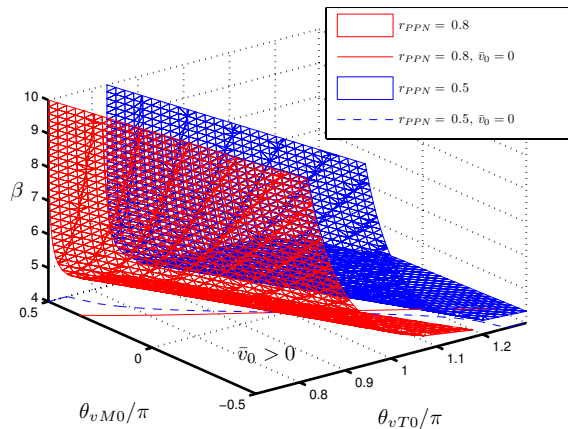


Fig. 9. Admissible Region of Finite LOS Turn Rate

## REFERENCES

- [1] T. Kuroda and F. Imado, "Advanced missile guidance system against very high speed target," *Journal of Guidance, Control and Dynamics*, pp. 320–324, 1988.
- [2] P. J. Yuan, "Anti-missile guidance," *A Report to Chun Shan Institute of Science and Technology*, pp. 1–6, 2007.
- [3] C. L. Lin and H. Z. Hung, "Development of an integrated fuzzy-logic-based," *IEEE Transactions on Fuzzy Systems*, vol. 12, no. 2, pp. 157–169, April 2004.

- [4] M. Guelman, "A Qualitative Study of Proportional Navigation," *IEEE Transactions on Aerospace and Electronic Systems*, vol. 3, pp. 337–343, July 1971.
- [5] K. Becker, "Closed-form solution of pure proportional navigation," *IEEE Transactions on Aerospace and Electronic Systems*, vol. 26, no. 3, pp. 526–533, 1990.
- [6] J.-H. Oh and I.-J. Ha, "Performance analysis of 3-dimensional PPNG law against a high speed target," in *Proceedings of the 36th Conference on Decision and Control*, vol. 4, San Diego, California, December 1997, pp. 3144–3149.
- [7] S. N. Ghawghawe and D. Ghose, "Pure proportional navigation against time-varying target manoeuvres," pp. 1336–1347, 1996, iD: 1.
- [8] F. Tyan, "Unified approach to missile guidance laws: A 3d extension," *IEEE Transactions on Aerospace and Electronic Systems*, vol. 41, no. 4, pp. 1178–1199, October 2005.
- [9] C. Y. Kuo and Y. C. Chlou, "Geometric analysis of missile guidance command," *Control Theory and Applications, IEE Proceedings -*, vol. 147, no. 2, pp. 205–211, 2000.
- [10] N. Dhananjay, D. Ghose, and M. S. Bhat, "Capturability analysis of a geometric guidance law in relative velocity space," in *American Control Conference, 2007. ACC '07*, 2007, pp. 4564–4569.
- [11] F. Tyan and J. F. Shen, "A simple adaptive gipn missile guidance law," *Proceedings of the 2006 American Control Conference*, pp. 345–350, June 2006.